

## Review

# Hepatic stellate cells: Three-dimensional structure, localization, heterogeneity and development

By Kenjiro WAKE<sup>†)</sup>

Emeritus Professor of Department of Anatomy, Faculty of Medicine,  
Tokyo Medical and Dental University, Tokyo, Japan

(Communicated by Kiyoshi HAMA, M. J. A.)

**Abstract:** Hepatic stellate cells (HSCs) are vitamin-A storing collagen-producing cells in hepatic lobules. The three-dimensional structure of HSCs has been demonstrated with the Golgi method, the maceration method for scanning electron microscopy, and confocal laser scanning microscopy. Many thorn-like microprojections or spines extend from the subendothelial processes and make contacts with hepatocytes. One HSC entwines two or more sinusoids and about 20-40 hepatocytes to create a cellular unit, 'the stellate cell unit' or 'stellon'. The Space of Disse is defined as the space between stellate cell-endothelial cell complex and hepatocytes. Intralobular heterogeneity of HSCs is assessed. HSCs develop from mesenchymal cells in the *septum transversum*. The developmental process of HSCs is reproduced partly in culture. In the lamprey abundant vitamin A is stored not only in HSCs, but in the fibroblast-like cells in the various other splanchnic organs. In vertebrates, the existence of both conventional fibroblast system in somatic tissues and vitamin A-storing cell system in splanchnic organs is suggested.

**Key words:** Hepatic stellate cells; 3-D structure; sinusoid; Space of Disse; heterogeneity; development.

**Introduction.** Hepatic stellate cells (HSCs) are mesenchymal cells in the hepatic lobule which store vitamin A and are the major cell type responsible for collagen production in liver fibrosis and cirrhosis. First described in gold chloride preparations of the liver as 'Sternzellen' by Carl von Kupffer in 1876,<sup>1)-3)</sup> the characterization of these cells began only 35 years ago.<sup>4)-9)</sup> Upon inflammation in the liver, these cells become activated, a process in which they lose vitamin A lipid droplets, proliferate, transform into myofibroblasts, and increase their synthesis of extracellular matrix proteins.<sup>10)-17)</sup> HSCs are generally considered to correspond to 'Ito cells (fat-storing cells)',<sup>5)</sup> 'vitamin A-storing cells',<sup>6)</sup> or 'pericytes in the liver'.<sup>18)</sup>

Our basic knowledge on morphology of HSCs remains limited. Once the three-dimensional structure of HSCs is elucidated, it will be easier to interpret cell-to-

cell interactions of liver cells and pathological alternations of the liver tissue. This mini-review provides overviews of HSC morphology, highlighting more recent studies on their 3-D structure, exact localization, including their intralobular heterogeneity, their ontogenetic development, and the presence of similar cells distributed widely in the splanchnic organs of the lamprey, *Lampetra japonica*. Detailed historical background and informations on earlier studies are referred to in previous reviews.<sup>2),3)</sup>

**Three-dimensional structure of hepatic stellate cells (HSCs) as revealed by different methods.** Since HSCs send characteristic long cytoplasmic processes which spread three-dimensionally, the entire view of the cell is best visualized using special methods. The data obtained by individual methods are as follows:

**A) Golgi method. a) Light microscopy.** The Golgi method was the first method introduced successfully for the 3-D demonstration of HSCs by Zimmermann.<sup>18)</sup> He described dendritic perisinusoidal cells ('Pericyten') with the Golgi-Kopsch chrome-silver

<sup>†)</sup> Present address: Liver Research Unit, Minophagen Pharmaceutical Co., Ltd., 8-10-22, Akasaka, Minato-ku, Tokyo 107-0052, Japan (wake@minophagen.co.jp).

method. We used the rapid Golgi method for the demonstration of HSCs of various animals.<sup>8),9)</sup> Upon application of this method, various cell types in the liver tissue stained deep brown in color non-specifically against a pale yellow background.<sup>19),20)</sup> The Golgi method has some advantages for analysis of the 3-D structure of HSCs; 1) structure of the cell is well preserved, because of the good perfusion fixation, and 2) a single cell profile is obtained with a high contrast which is convenient for morphological analysis. By this staining property, it is rather easy to recognize the spreading area of an individual HSC. HSCs can easily be discerned by their characteristic morphology.

HSCs display spindle-shaped, angular or rounded cell bodies and long cytoplasmic processes, which are categorized into two types; subendothelial processes and intersinusoidal processes (Fig. 1). The former processes extend from the cell body and course along the surface of sinusoidal endothelial cells and throw off numbers of long slender secondary branches which encircle the sinusoid at rather regular intervals. The outstanding feature of these processes is thorny microprojections or 'spines', which project from lateral edges of subendothelial processes. The latter processes project from the cell body or from stems of the former and follow their vertical course through the interhepatocellular space toward the neighboring two or three sinusoids.<sup>9),20)</sup> The surface of these processes are smooth, lacking spines. Once the tips of these processes reach the wall of a neighboring sinusoid, they expand into several perisinusoidal processes. Individual stellate cells may supply intersinusoidal processes to two or more neighboring sinusoids, tying them into a bundle.

**i) Stereo-pair microscopy.** Stereo-pair photographs of a single stellate cell obtained using the BH-2 stereo-microscopic apparatus (Olympus, Tokyo) shows their entire profile three-dimensionally.<sup>21)</sup>

**ii) Video-presentation of the computer-aided rotating images.** The Golgi-stained liver tissue is embedded in an epoxy resin (Epon 812), and serially sectioned to produce 1-2  $\mu\text{m}$  thick sections, using a HistoDiamond knife mounted on a rotary microtome.<sup>22)</sup> The video-output signal is directly fed into the computer (C2000DIPS, Hamamatsu Photonics). The image demonstrates not only a simple stacked profile of the cell, but also its side view by rotation in video presentation (Figs. 2A-C). The technology confirms that the every HSC surrounds the sinusoid with subendothelial processes.

Using above various methods, entire profiles of

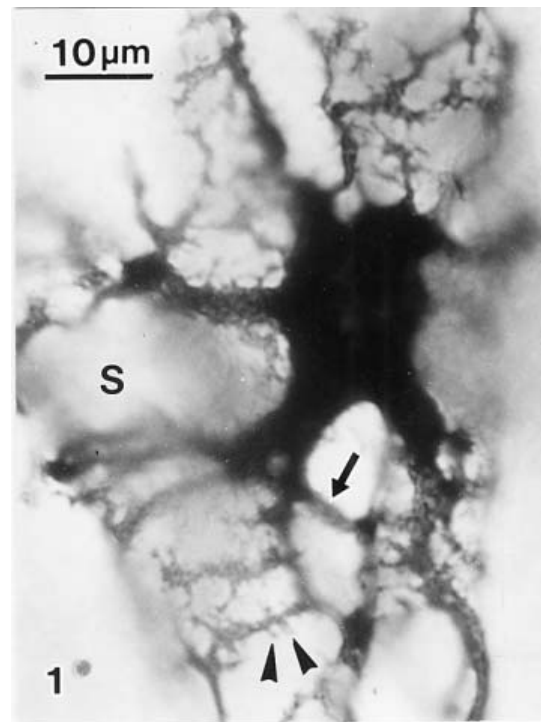


Fig. 1. A hepatic stellate cell (HSC) of the rat liver sends long and branching subendothelial processes decorated with numerous spines (arrowhead) to three sinusoidal walls. An intersinusoidal process (arrow) extends from a thick branch. S: sinusoid. Rapid Golgi silver method  $\times 1400$ .

two HSCs of the porcine liver are depicted in Fig. 3.

**b) Electron microscopy. i) Backscattered electron imaging by SEM.** Golgi-sections, 50  $\mu\text{m}$  in thickness, of the liver are subjected to critical point-drying and are examined by SEM in the backscattered mode.<sup>20)</sup> By silver being heavily precipitated on the processes of HSCs, the subendothelial processes with thorny outline, which lie on the abluminal surface of the endothelial cells, can be observed through transparent wall of endothelium from the luminal surface. Lowering the accelerating voltage adequately will unmask the overlapped images of opposing semitransparent endothelial cells and subendothelial process of the HSCs.<sup>9)</sup>

**ii) High-voltage electron microscopy (HVEM).** The Golgi-stained preparations are re-embedded in Epon, cut 4  $\mu\text{m}$  thick, and examined with a HVEM at an accelerating voltage of 1000 kV.<sup>9)</sup> Numerous spines, which are more or less impregnated, protruded laterally through out the whole length of perisinusoidal processes. Some spines projecting from the neighboring subendothelial processes may fuse together and bridge subendothelial processes to make a

fine network. The outer surface of the sinusoidal endothelium is, therefore, covered for the most part with an extensive and intricate meshwork of numerous fine processes extending from HSCs.

**iii) Maceration method for SEM.** This sophisticated technique provides a remarkably wider view of HSCs under SEM.<sup>9),23),24)</sup> Careful SEM observation reveals that spines extend from the lateral edges of subendothelial processes and course obliquely through the Space of Disse away from the abluminal surface of the endothelial cells to make contacts with the plasma membrane of hepatocytes (Figs. 4 and 5). The cell membrane of the subendothelial process adhered to the endothelial cell is smooth, while the outer cell membrane of the opposite side is decorated by short microvillous projections (Fig. 5). The stellate cell-hepatocyte contact is observed by the routine transmission electron microscopy of thin sections (Fig. 4. Inset).<sup>24)</sup> The opposing cell membranes at these contacts, especially of the hepatocytes are reinforced on the cytoplasmic surface by moderately dense materials of a fine filamentous nature. Therefore, HSCs adhere to sinusoidal endothelial cells on the one hand and to hepatocytes on the another one.

**B) Cytochemical methods for confocal laser scanning microscopy.** Cell bodies and the cytoplasmic processes of HSCs contain desmin,<sup>25)</sup>  $\alpha$ -smooth muscle actin ( $\alpha$ -SMA)<sup>26)</sup> and glial fibrillary acidic protein (GFAP).<sup>27)</sup> These cytoskeletal proteins generally have been used for markers of HSCs in the normal and injured liver tissues, but not all of HSCs are positive, e.g., desmin is positive in 70-80% of the rat liver.<sup>28)</sup> HSCs in the normal human liver are desmin negative.<sup>14)</sup>  $\alpha$ -SMA is negative in normal rat HSCs and becomes positive when HSCs are activated.<sup>26)</sup> Twenty to thirty% of rodent HSCs and normal human HSCs are GFAP-negative.<sup>29)</sup>

Oikawa and his group<sup>30)</sup> demonstrated the 3-D structure of HSCs with cytochemistry of GFAP using confocal laser scanning microscopy. This method is stable compared with the classical Golgi method, but reveals no fine cytoplasmic processes without filamentous bundles, showing very different features from those stained with the Golgi method.

**Localization of HSCs and a novel definition of 'the Space of Disse'.** From the data obtained by various methods and techniques, the 3-D structure of HSCs as well as the relationship between HSCs and other sinusoidal elements are illustrated in the model shown in Fig. 2D. Collagen fibrils and nerve fibers course in the

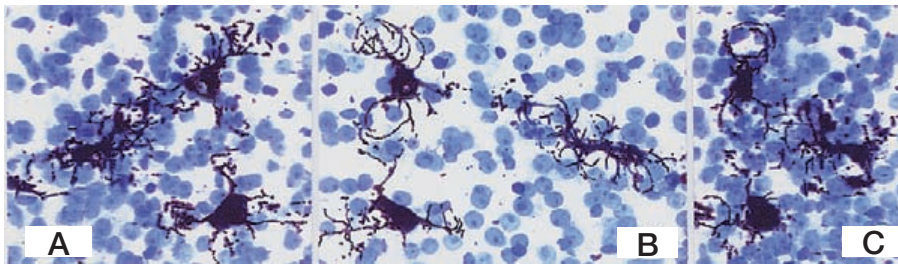
Space of Disse outside of the endothelial cell-HSC complex.

HSCs are distributed within hepatic lobules, adhering to sinusoidal endothelial cells with long subendothelial processes to generate the endothelial cell-HSC complex. Basement membrane-like substance is seen in the intercellular cleft (20 nm in width) between both cells (Fig. 2E). The thorn-like microprojections (spines) which project out from the lateral edges of subendothelial processes stand up from the surface of the outer surface of the endothelial cells crossing the Space of Disse to contact with the cell membrane of the hepatocyte.<sup>24)</sup> The contacting area of the hepatocytes shows a membrane thickening to which microfilaments converge (Fig. 4, inset). Thus, HSCs make contacts with both endothelial cells and hepatocytes. Collagen fibrils and nerve fibers course in the Space of Disse outside of the endothelial cell-HSC complex (Figs. 2D and 2E).

Textbooks describe the Space of Disse to be the space external to the sinusoidal endothelial cells and that HSCs are situated *within* the Space of Disse. However, based on our observations, the Space of Disse is newly defined as the space between the endothelial cell-HSC complex and hepatocytes, containing collagen fibrils and nerve fibers, being bridged by many thorn-like microprojections of HSCs (Fig. 2E).

**A possible role of HSCs in the sinusoidal flow.** In culture, HSCs contract in response to thromboxane-A<sub>2</sub> analog, prostaglandin F<sub>2</sub>, endothelin-1, substance P<sup>31)-33)</sup> and relax in response to PGI<sub>2</sub> analog, prostaglandin E<sub>2</sub>, and NO.<sup>31)</sup> Since cultured HSCs are activated and changed to myofibroblasts, the data do not appear to indicate the contractility of the normal (quiescent) HSCs *in vivo*. On the other hand, *in vivo* microscopy has demonstrated contraction of sinusoids in response to endothelin-1.<sup>34)</sup> Histological observation after endothelin-1 perfusion via the portal vein, the presinusoidal segment of the portal vein is most significantly constricted, and sinusoids are only mildly constricted.<sup>35)</sup> In these *in vivo* perfusion experiments, it is difficult to discriminate whether the contraction is due to terminal muscle cells or HSCs. The problem concerning the regulation of sinusoidal blood flow by quiescent HSCs in the normal liver remains to be elucidated. The contractile potential of activated HSCs after liver injury is markedly enhanced.<sup>36)</sup>

Another possible function of quiescent HSCs appears to be in the local control of sinusoidal tone or elasticity to regulate the fluid exchange between the lumen of sinusoid and the Space of Disse through



Figs. 2A-C. A series of rotating images of three HSCs in a liver lobule of the pig. A: 0° ; B: 120°; C: 180° Golgi silver method. The sections are stained with toluidine blue. × 350.

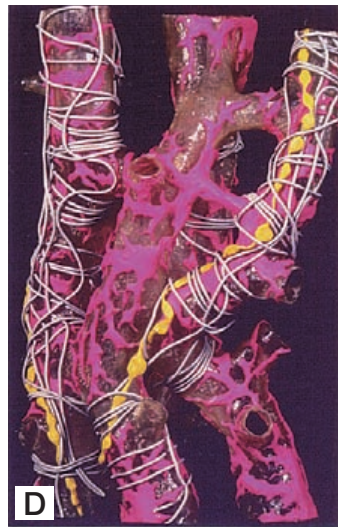


Fig. 2D. A plastic model of the sinusoidal wall of the rat liver. Red: HSC; yellow: nerve fibers, gray: collagen fibers. Note the layered arrangement of sinusoidal elements.

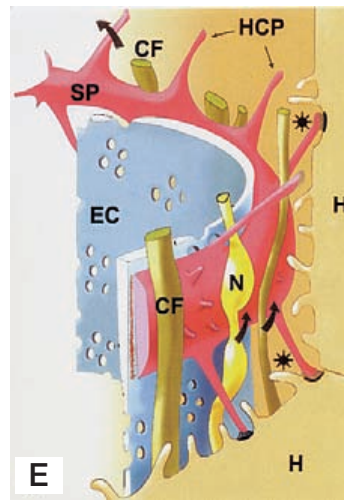


Fig. 2E. A schematic representation of the sinusoidal wall. Arrows indicate the tunnel made with the subendothelial processes (SP), hepatocyte-contacting process (HCP, spine), and hepatocytes (H). The tunnel contains collagen fibers (CF) and nerve fibers (N). EC: endothelial cell; Asterisks: Space of Disse.

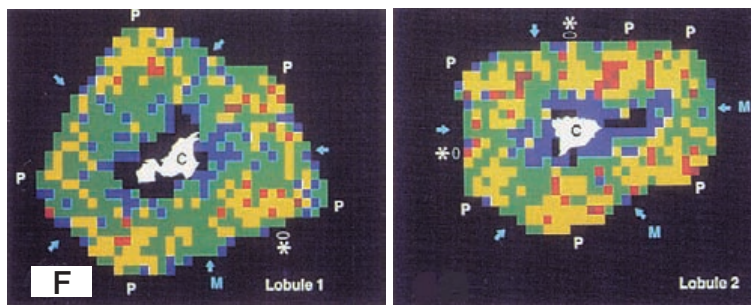


Fig. 2F. The mapping of lobule 1 and lobule 2 depicts the average value of vitamin A-containing lipid droplets of the porcine stellate cells graded 5 levels of coloring: 1-20 μm<sup>2</sup> (blue) ; 21-40 μm<sup>2</sup> (green); 41-60 μm<sup>2</sup> (yellow); 61-80 μm<sup>2</sup> (red); and 81 μm<sup>2</sup> (brown). Vitamin A-storing profile in the lobule 2 is higher than the lobule 1. Intralobularly, low values (blue and green) are encountered especially in the centrilobular zones. High values (red and brown) emerge as a concentration near the corners with portal tract (P), and spread over toward the midseptum (M, arrows) and less toward the central vein (C). In addition to the corner portal branch, a septal portal branch could be identified (asterisk); there, the adjacent values tend to be heightened. (From ref. 44. Reprinted by permission).

endothelial fenestrae.<sup>24),37)</sup> For the fluid exchange through endothelial fenestrae, Wisse and his group<sup>38)</sup> reported two concepts, 'forced sieving' and 'endothelial massage', which are based on the effect of flowing white blood cells whose diameters are larger than those of sinusoids.

Another possible concept for the contribution of fluid exchange through fenestrae is 'pumping mechanism'.<sup>24),37)</sup> Mechanical roles of obliquely arranged spines of HSCs in the Space of Disse may generate not only elasticity of the sinusoidal wall, but also opening and shutting of intercellular recesses of hepatocytes. In the relaxation phase of HSCs or when the sinusoidal wall is compressed by blood cells, the Space of Disse becomes narrow, elevating the pressure of the Space of Disse, particles and fluid in the Space of Disse are pushed out into the sinusoidal lumen. While, in contraction phase of HSCs without compression of the sinusoidal wall, the recesses open and the Space of Disse expands effectively, reducing the pressure of the Space of Disse, particles and fluid are absorbed into the Space of Disse.

**The stellate cell unit: 'The stellation'.** The nucleus-to-nucleus distance of HSCs resided on sinusoids is  $70.6 \pm 9.8 \mu\text{m}$  in the rat liver.<sup>39)</sup> While the average length of a single endothelial cells is  $83.99 \pm 3.39 \mu\text{m}$  in the centrilobular zone and  $76.65 \pm 2.25 \mu\text{m}$  in the periportal area.<sup>40)</sup> A single HSC sends branching cytoplasmic processes to two, three, and sometimes more neighboring sinusoids. Conversely, a single endothelial cell receives cytoplasmic processes from one to three HSCs. On the other hand, subendothelial processes of a single HSC appear to make contacts through their spines with 20-40 hepatocytes. The endothelial cell-stellate cell-hepatocyte (cell to cell to cell) complex may create a cellular unit in the liver tissue. We call this unit 'the stellate cell unit', or in brief '*the stellation*'. The stellation is not an independent unit, but a loosely overlapping unit with neighboring units as shown in Fig. 6.

The intimate association between HSCs and the neighboring cell types through the stellation may facilitate intercellular transport and paracrine stimulation by soluble mediators. For example, the retinol-retinol binding protein (RBP) complex released from a number of hepatocytes<sup>41)</sup> is transported to a smaller number of stellate cells, being the condensing manner (*convergence*). Convergent intercellular communication may occur in proliferation of HSCs by 60 kD protein released from normal or injured hepatocytes.<sup>42)</sup> In the same manner, contraction/relaxation of activated HSCs are influenced by endothelin/NO released from

endothelial cells.<sup>31),32),36)</sup> When HSCs contract or relax, sinusoidal endothelial cells are contracted or relaxed. This wavy motion of HSCs is conducted to increased number of endothelial cells and hepatocytes in a *spreading* manner. Tumor-activated HSCs release proliferation- and tubulization-stimulating factors to sinusoidal endothelial cells.<sup>43)</sup> The effects of this releasing also may be defined as *spreading*. From the above mentioned cell-to-cell-to-cell relations, the stellation may be a transducer coupled between the blood stream and the hepatic parenchyma which regulates various functions and pathologies in the liver.

**Intralobular heterogeneity of HSCs.** HSCs display marked morphological zonal heterogeneity,<sup>20)</sup> desmin-immunoreactivity<sup>20),28)</sup> and vitamin A-storage.<sup>20),44),45)</sup> In the porcine liver, the widened sinusoids are accompanied by HSCs bearing longer dendritic processes with more thorn-like microprojections, in comparison to those projecting from periportal elements.<sup>20)</sup> Oikawa and his group<sup>30)</sup> reported using the GFAP-immunostaining that cytoplasmic processes of rat HSCs were longer in the mid zone than those in periportal and pericentral zones.

HSCs and sinusoidal endothelial cells spread widely to magnify their surface areas by arborizations in the former and fenestrations in the latter. As the result, the comparative surface areas of perinuclear thick portions containing nuclei in the sinusoidal wall are limited. These facts may be favorable for fluid exchange between the Space of Disse and the blood stream in the sinusoid. Generally cells forced to extend themselves over a large surface survive better and proliferate faster than cells with more rounded shape.<sup>46)</sup> Accordingly the HSCs in the centrolobular area which spread more widely may thrive than those cells in the periportal area.

Desmin immunoreaction in the periportal zones is stronger than that in the centrolobular zones in the porcine liver.<sup>20)</sup> Vitamin A-storage in the HSCs is well developed in the vicinity of periportal region, but diminishes gradually toward the central vein and may almost disappears in the central zone.<sup>20),44),45)</sup> Zou *et al.* (1998)<sup>44)</sup> showed that vitamin A-storage in HSCs varies not only with cell location along the sinusoidal axis but also with the origin of the sinusoid; sizes of vitamin A-containing lipid droplets of an individual HSC change from region to region within the same zones (Fig. 2F). Values were significantly higher at periportal than mid-septal regions (origins of their sinusoids are located at the midpoint of the portal-to-portal (p-p) interlobular septum). Along the periphery, inlet venules are quanti-

fied, revealing in occurrence rate of 60% at periportal, and 5% at midseptal regions. These values are closely compatible with the regional gradient of vitamin A-storage. Thus, vitamin-A storage in HSCs is related to the portal vasculature in the liver.

**Development of HSCs.** Concerning the origin of the HSC, a dispute exists on the question of whether the primordial cells arise from the mesenchymal cells in the *septum transversum*<sup>47)</sup> or from the neural crest cells. The latter possibility is based on the findings that HSCs contain nervous-tissue-associated proteins such as N-CAM,<sup>48)</sup> cellular prion protein,<sup>49)</sup> synaptophysin,<sup>50)</sup> RhoN<sup>51)</sup> and GFAP.<sup>27)</sup>

We infer from light and electron microscopic observations (unpublished data) that mesenchymal cells in the *septum transversum* give rise to HSCs in the early embryonic stages. At the Carnegie stage 13 (4-5 mm body length of a human fetus), a wide zone of the mesenchymal tissue containing primordial HSCs is

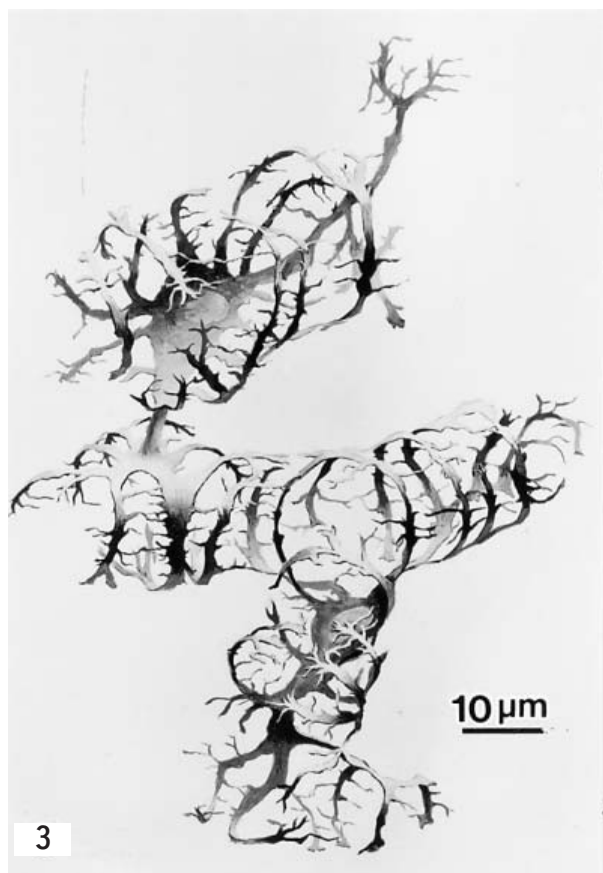


Fig. 3. Drawing of the three-dimensional structure of two HSCs of a pig, from findings obtained by the Golgi method. (From ref. 37. Reprinted by permission)  $\times 1000$ .

intercalated between the capillary and the developing hepatic cell cord. After a short period, these cells become sandwiched tightly between the capillary endothelium and the hepatic cell cord. In addition, in the lower vertebrates, e.g., lamprey, as shown in the following chapter, the vitamin A-storing cells are all of the fibroblasts in the splanchnic organs of the animal. From these findings, the nervous origin of HSCs from the neural crest appears to be doubtful.

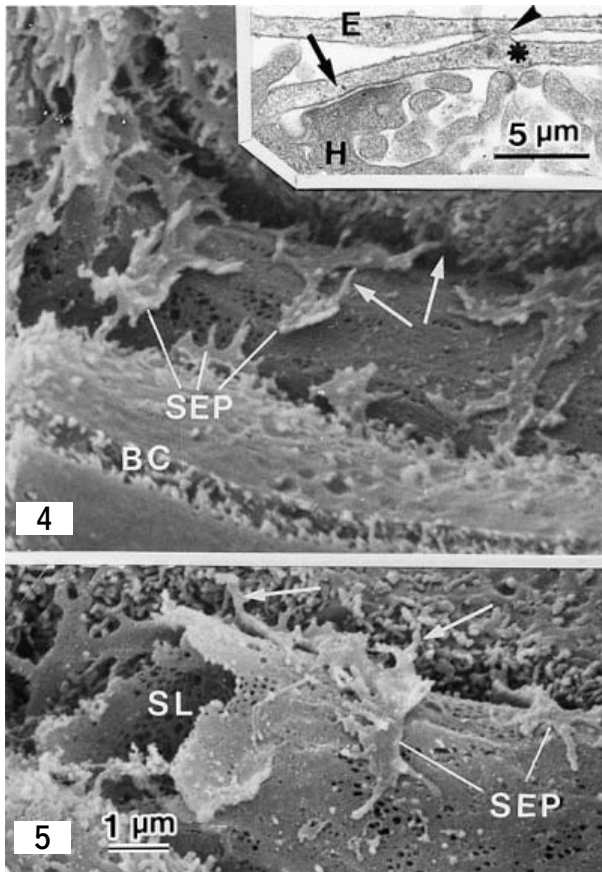
Postnatal development of the HSC in the rat liver was demonstrated by the Golgi method (Figs. 7A-D).<sup>52)</sup> Cytoplasmic processes of HSC develop rapidly during early postnatal stages. In one-day old rat, the cells are rather rounded with slim and scanty processes. At week 1 and 2 they come to conform with the longitudinal axis of the sinusoid, roughly fusiform in shape. Primary processes branch out from the cell body proximally and distally with abundance of secondary processes extending to embrace the sinusoidal tubes. At week 2 and 3 the cell processes extend even longer and are expanded. Apparently an intercellular contact is established between hepatocytes' plasma membrane and stellate cells' thorny micropjections. Cell growth continues steadily up to at least week 5. Vitamin A lipid droplets are scant in the neonate, but they increased constantly with age both in terms of number and size. In the perinatal rats, HSCs are involved in the blood-forming colonies.<sup>52)</sup>

There is little doubt that HSCs have not achieved their final form when the animal is born. Their characteristic arborization of cytoplasmic processes studded with spines develops rapidly after birth and differentiates steadily as the animal grows. As a consequence in lobular expansion, the radial sinusoids elongate. It seems natural to perceive that the HSCs, which form an uninterrupted pericytic layer encasing each sinusoid from peripheral to central ends, would be similarly involved in the growing process.

Video-observations of cultured HSCs show that on plastic, HSCs extend thin fan-shaped membranous processes around the nuclei. As these membranous processes expand further, the processes assume a dendritic form toward the peripheral portion of the processes (Figs. 7E-G).

**HSCs in the lower vertebrate, lampreys.** It is well known that the lamprey, *Lampetra japonica*, store much vitamin A during the period of the spawning migration. Accordingly, the lamprey's HSC might be an interesting comparative subject for liver research.

HSC of the lamprey contains many large lipid



Figs. 4 and 5. Scanning electron micrographs showing the Space of Disse and spines (arrows) of HSCs of the rat liver. Spines project from lateral edges of the subendothelial processes (SEP) course obliquely through the Space of Disse and contact with hepatocytes. BC: bile canaliculus; SL: sinusoidal lumen.  $\times 8,000$ . Fig. 4 inset: A transmission electron micrograph of a longitudinal section of the spine which extends from the subendothelial process (asterisk). The spine, crossing the Space of Disse, adheres to both an endothelial cell (E) (arrowhead) and a hepatocyte (arrow).  $\times 24,000$  (Fig. 5 from ref. 62, Reprinted by permission).

droplets, which occupy most of the cytoplasm.<sup>53,54</sup> In the lamprey liver, they are seen not only in the lobule, but also in the interstitial connective tissues; the 'fibroblast-like' elements in the dense interstitial connective tissue in the fibrous capsule, perivascular interstitium as well as in the hilar formations contain abundant vitamin A lipid droplets. Since the organization of the hepatic cell cord is not yet well developed in the lower vertebrates, HSCs associated with collagen fiber bundles are arranged irregularly. However, some branching processes of the individual HSC appear to attach to sinusoidal endothelial cells. Characteristic components of lamprey HSCs are

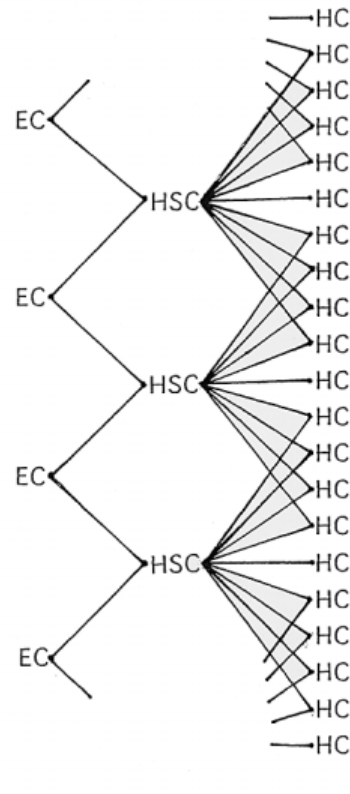
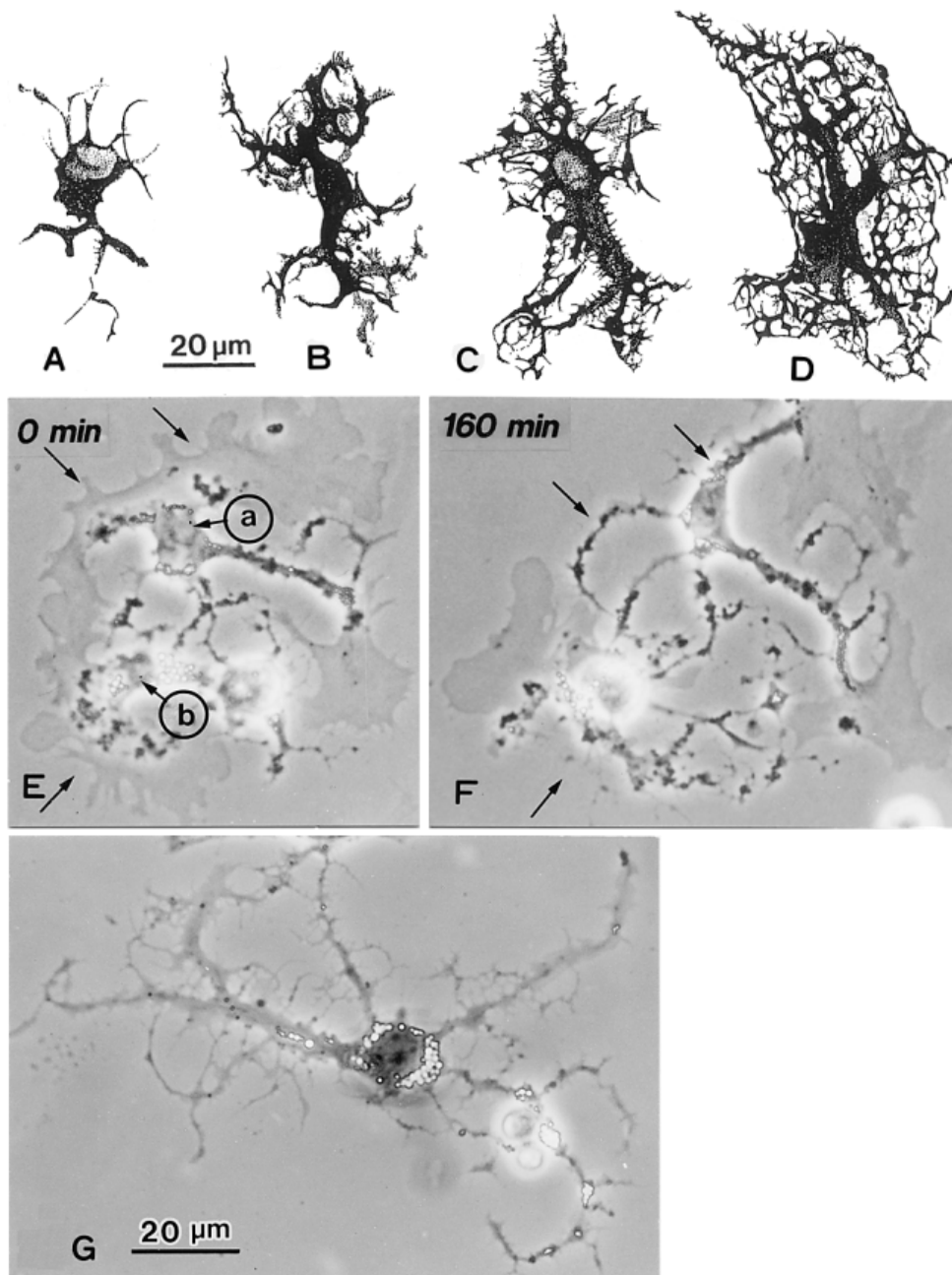


Fig. 6. Schematic representation of the 'stellon' (stellate cell unit) consisted of a HSC, endothelial cells (EC), and hepatocytes (HC). (see text).

large lipid droplets in the cytoplasm; the membrane-bounded lipid droplets (Type I lipid droplets)<sup>52</sup> are scarcely seen. Lysosome-like dense bodies are frequently seen in the cytoplasm, but no multivesicular bodies.

Similar cells storing vitamin A are present in other splanchnic organs of the lamprey; intestine,<sup>2),56)</sup> gill,<sup>56),57)</sup> kidney,<sup>2),56),58)</sup> and heart.<sup>2),56)</sup> We propose as a hypothesis that these cells belong to the stellate cell system (family) that stores vitamin A and regulates homeostasis of the vitamin in the whole body in the lamprey. Fibroblastic cells in the skin and somatic muscle of the lamprey stored little vitamin A.

In mammals, vitamin A is stored not only in the HSCs, but also in fibroblastic cells in various splanchnic organs.<sup>6),7)</sup> Cytochrome/stellate cell activation-associated protein (Cytochrome/STAP),<sup>59),60)</sup> which is detected only in the splanchnic fibroblastic cells (stellate cell system) and not in the somatic fibroblasts.<sup>61)</sup> These results indi-



Figs. 7A-D. Postnatal development of HSCs of the rat. Camera-lucida drawing of Golgi-preparations in rats age 1 day (A), 1 week (B), 3 weeks (C) and 5 weeks (D).  $\times 600$ .

Figs. 7E-G. *In vitro* development of hepatic stellate cells isolated from the rat liver. E. After seeding, two cells a and b extend membranous processes around cell bodies. The membranous processes are changing to dendritic in appearance remaining the peripheral regions. After 160 min (F) spines are formed (arrows). G. Twenty-four hours after seeding, dendritic branches with spines develop. Vitamin A-lipid droplets (clear spots) are distributed in the cell body, some of which are seen in the processes. (Figs. 7A-D from ref. 62. Reprinted by permission).  $\times 700$ .

cate that splanchnic mesenchyma is different from that of somatic tissues in vertebrates.

**Concluding remarks.** The three-dimensional structure of HSCs has been demonstrated by various staining methods using light and electron microscopy. Two different kinds of cytoplasmic processes are differentiated, the subendothelial processes and intersinusoidal processes. The former encompass sinusoidal endothelial cells with their long subendothelial processes, adhering to the endothelial cells. These processes are characterized by thorn-like microprojections (spines), which are project from the lateral edge of individual subendothelial processes and contact with hepatocytes. Thus, HSCs are intercalated between endothelial cells and hepatocytes. These three-kinds of cells generate the cell-chain unit, called 'stellon', and may play an important role in intercellular cross talk or transport.

Intralobular heterogeneity of HSCs is recognized. HSCs are derived from the mesenchymal cells in the *septum transversum* and extend cytoplasmic processes rapidly after birth. *In vitro*, the fan-shaped membranous process of isolated HSCs changes to dendritic appearance after seeding. In the lamprey liver, the mesenchymal cells of various splanchnic organs in the lamprey, storage of abundant vitamin A is concentrated in the splanchnic organs. From these findings, the mesenchyma in the body may be differentiated into splanchnic and somatic ones in vertebrates.

**Acknowledgements.** The author appreciates Dr. Robert S. McCurskey, Department of Cell Biology and Anatomy, College of Medicine, University of Arizona, for reviewing the manuscript.

### References

- 1) von Kupffer, C. (1876) Arch. Mikr. Anat. **12**, 353-358.
- 2) Wake, K. (1980) *In* Int. Rev. Cytol. (eds. Bourne, G. H., and Danielli, J. F.). Vol. 66, Academic Press, New York, pp. 303-353.
- 3) Wake, K. (2004) Comp. Hepatol. **3** (Suppl. D), S2.
- 4) Wake, K. (1971) Am. J. Anat. **132**, 429-461.
- 5) Ito, T. (1973) Gumma Rep. Med. Sci. **6**, 119-163.
- 6) Yamada, E., and Hirotsawa, K. (1976) Cell Struct. Funct. **1**, 201-204.
- 7) Kusumoto, Y., and Fujita, T. (1977) Arch. Histol. Jpn. **40**, 121-136.
- 8) Wake, K., Motomatsu, K., and Senoo, H. (1987) Cell Tissue Res. **249**, 289-299.
- 9) Wake, K. (1988) *In* Biopathology of the Liver. An Ultrastructural Approach (ed. Motta, P. M.). Kluwer Acad. Pub., Dordrecht, pp. 23-36.
- 10) Blomhoff, R., and Wake, K. (1991) FASEB J. **5**, 271-277.
- 11) Bissel, D. M. (1992) Gastroenterology **102**, 1803-1805.
- 12) Friedman, S. L. (1993) New Engl. J. Med. **328**, 1828-1835.
- 13) Hautekeete, M. L., and Geerts, A. (1997) Virchow. Arch. **430**, 195-207.
- 14) Kawada, N. (1997) Histol. Histopathol. **12**, 1069-1080.
- 15) Friedman, S. L. (2000) J. Biol. Chem. **275**, 2247-2250.
- 16) Friedman, S. L. (2001) The Hepatic Stellate Cell. *In* Seminars in Liver Diseases (ed. Berk, P. D.). Vol. 21, No. 3, Thieme, New York, pp. 307-459.
- 17) Senoo, H. (2004) Med. Electron Microsc. **37**, 3-15.
- 18) Zimmermann, K. W. (1923) Z. f. ges. Anat. **68**, 29-109.
- 19) Wake, K. (1989) *In* Cells of the Hepatic Sinusoid (eds. Wisse, E., Knook, D. L., and Decker, K.). Vol. 2, Kupffer Cell Foundation, Rijswijk, The Netherlands, pp. 449-450.
- 20) Wake, K., and Sato, T. (1993) Cell Tissue Res. **273**, 227-237.
- 21) Wake, K. (1989) *In* Cells and Tissues: A Three Dimensional Approach by Modern Techniques in Microscopy (ed. Motta, P. M.). Alan R. Liss. Inc., pp. 257-262.
- 22) Koike, H., Imanishi, M., and Umitsu, Y. (1996) *In* Basic Neuroscience in Invertebrates (eds. Koike, H., Kidokoro, Y., Takahashi, K., and Kanaseki, T.). Japan Sci. Soc. Press, Tokyo, pp. 293-312.
- 23) Takahashi-Iwanaga, H., and Fujita, T. (1986) Arch. Histol. Japan **49**, 349-357.
- 24) Wake, K. (1995) *In* Cells of the Hepatic Sinusoid (eds. Wisse, E., Knook, D. L., and Wake, K.). Vol. 5, Kupffer Cell Foundation, Leiden, The Netherlands, pp. 241-246.
- 25) Yokoi, Y., Namihisa, T., Kuroda, H., Komatsu, I., Miyazaki, A., Watanabe, S., and Usui, K. (1984) Hepatology **4**, 709-714.
- 26) Ramadori, G., Veit, S., Schwögler, H. P., Dienes, T., Knittel, H., Rieder, H., and Meyer zum Büschenfelde, K.-H. (1990) Virchows Arch. B Cell Pathol. **59**, 349-357.
- 27) Niki, T., DeBleser, P. J., Xu, G., Van den Berg, K., Wisse, E., and Geerts, A. (1996) Hepatology **23**, 1538-1545.
- 28) Ballandini, G., Groff, P., DeGiorgi, L. B., Schuppan, D., and Bianchi, F. B. (1994) Hepatology **19**, 440-446.
- 29) Levy, M. T., McCaughan, G. W., Abbott, C. A., Park, J. E., Cunningham, A. M., Mueller, E., Rettig, W. J., and Gorrell, M. D. (1999) Hepatology **29**, 1768-1778.
- 30) Oikawa, H., Masuda, T., Kawaguchi, J., and Sato, R. (2002) J. Gastroenterol. Hepatol. **17**, 861-872.
- 31) Kawada, N., Klein, H., and Decker, K. D. (1992) Biochem. J. **285**, 367-371.
- 32) Kawada, N., Tran-Thi, T.-A., Klein, H., and Decker, K. (1993) Eur. J. Biochem. **213**, 815-823.
- 33) Sakamoto, M., Ueno, T., Kin, M., Ohira, H., Torimura, T., Inuzuka, S., Sato, M., and Tanikawa, K. (1993) Hepatology **18**, 978-983.
- 34) Bauer, M., Zhang, J. X., Bauer, I., and Clemens, M. G. (1994) Am. J. Physiol. Gastrointest. Liver Physiol. **267**, 143-149.
- 35) Kaneda, K., Ekataksin, W., Sogawa, M., Matsumura, A., Cho, A., and Kawada, N. (1998) Hepatology **27**, 735-747.
- 36) Rockey, D. C. (2001) *In* The Hepatic Stellate Cell (ed. Friedman, S. L.) Seminars in Liver Disease **21**, pp. 337-349.
- 37) Wake, K. (1996) *In* Functional Heterogeneity of Liver Tissue

- (ed. Vidal-Vanaclocha, F). Springer, New York, R. G. Landes, Austin, pp. 57-67.
- 38) Wisse, E., De Zanger, R. B., Charels, K., Van Der Smissen, P., and McCuskey, R. S. (1985) *Hepatology* **5**, 683-692.
- 39) Wake, K. (1982) *In Sinusoidal Liver Cell* (eds. Knook, D. L., and Wisse, E. ). Elsevier, Amsterdam, pp. 1-12.
- 40) Wake, K., Motomatsu, K., Dan, C., and Kaneda, K. (1988) *Cell Tissue Res.* **253**, 563-571.
- 41) Blomhoff, R., Green, M., Green, J. B., Berg, T., and Norum, K. R. (1991) *Physiol. Rev.* **71**, 951-990.
- 42) Gressner, A. M., Brenzel, A., Lahme, B., Gressner, G., and Schlegel, E. (1993) *In Cells of the Hepatic Sinusoid* (eds. Knook, D. L., and Wisse, E.). Vol. 4, Kupffer Cell Foundation, Leiden, The Netherlands, pp. 231-234.
- 43) Santisteban, A., Olasso, E., Bidaurrazaga, J., Rosenbaum, J., and Vidal-Vanaclocha, F. (1999) *In Cells of the Hepatic Sinusoid* (eds. Wisse, E., Knook, D. L., de Zanger, R., and Fraser, R.). Vol. 7, Kupffer Cell Foundation, Leiden, The Netherlands, pp. 41-42.
- 44) Zou, Z., Ekataksin, W., and Wake, K. (1998) *Hepatology* **27**, 1098-1108.
- 45) Higashi, N., and Senoo, H. (2003) *Anat. Rec. Part A* **271**, 240-248.
- 46) Chen, C. S., Mrksich, M., Huang, S., Whitesides, G. M., and Ingber, D. E. (1997) *Science* **276**, 1425-1428.
- 47) Yamamoto, M., and Enzan, H. (1975) *Rec. Adv. RES Res.* **15**, 54-75.
- 48) Nakatani, K., Seki, S., Kawada, N., Kobayashi, K., and Kaneda, K. (1996) *Cell Tissue Res.* **283**, 159-165.
- 49) Ikeda, K., Kawada, N., Wang, Y. Q., Kadoya, H., Nakatani, K., Sato, M., and Kaneda, K. (1998) *Am. J. Pathol.* **153**, 1965-1700.
- 50) Cassiman, D., van Pelt, J., De Vos, R., Van Lommel, F., Desmet, V., Yap, S. H., and Roskaqms, T. (1999) *Am. J. Pathol.* **155**, 1831-1839.
- 51) Nishi, M., Takeshima, H., Houtani, T., Nakagawara, K., Noda, T., and Sugimoto, T. (1999) *Brain Res. Mol. Brain Res.* **67**, 74-81.
- 52) Wake, K., Motomatsu, K., and Ekataksin, W. (1991) *In Cells of the Hepatic Sinusoid* (eds. Wisse, E., Knook, D. L., and McCuskey, R. S.). Vol. 3, Leiden, The Netherlands, pp. 269-275.
- 53) Wake, K., and Senoo, H. (1986) *In Cells of the Hepatic Sinusoid* (eds. Kim, A., Knook, D. L., and Wisse, E.). Vol. 1, Kupffer Cell Foundation, Rijswijk, The Netherlands, pp. 215-220.
- 54) Wake, K., Motomatsu, K., and Senoo, H. (1987) *Cell Tissue Res.* **249**, 289-299.
- 55) Wake, K. (1974) *J. Cell Biol.* **63**, 683-691.
- 56) Wold, H. L., Wake, K., Higashi, N., Wang, D., Kijima, N., Imai, K., Blomhoff, R., and Senoo, H. (2004) *Anat. Rec. Part A* **276**, 134-142.
- 57) Wake, K., Sato, T., Ekataksin, W., and Kaneda, K. (1989) *Biomed. Res.* **10** (Suppl. 3), 597-605.
- 58) Bauer, P., and Wake, K. (1996) *Arch. Histol. Cytol.* **59**, 71-78.
- 59) Kawada, N., Kristensen, D. B., Asahina, K., Nakatani, K., Minamiyama, Y., Seki, S., and Yoshizato, K. (2001) *J. Biol. Chem.* **276**, 25318-25323.
- 60) Asahina, K., Kawada, N., Kristensen, D. B., Nakatani, K., Seki, S., Shiokawa, M., Tatenno, C., Obara, M., and Yoshizato, K. (2002) *Biochim. Biophys. Acta* **1577**, 471-475.
- 61) Nakatani, K., Okuyama, H., Shimahara, Y., Saeki, S., Kim, D. H., Nakajima, Y., Seki, S., Kawada, N., and Yoshizato, K. (2004) *Lab. Invest.* **84**, 91-101.
- 62) Wake, K. (1994) *In Fat-storing Cells and Liver Fibrosis* (eds. Surrenti, C., Casini, A., Milani, S., and Pinzani, M.). Kluwer Academic Publishers, Dordrecht, pp. 1-10.

(Received March 29, 2006; accepted April 12, 2006)